

Single-photon scattering and quantum entanglement of two giant atoms with azimuthal angle differences in a waveguide system

Jin-Song Huang(黄劲松), Hong-Wu Huang(黄红武), Yan-Ling Li(李艳玲), and Zhong-Hui Xu(徐中辉)

Citation: Chin. Phys. B, 2024, 33 (**5**): 050506. DOI: 10.1088/1674-1056/ad2508
Journal homepage: http://cpb.iphy.ac.cn; http://iopscience.iop.org/cpb

What follows is a list of articles you may be interested in

A thermal conductivity switch via the reversible 2H-1T' phase transition in monolayer $MoTe_2$

Dingbo Zhang(张定波), Weijun Ren(任卫君), Ke Wang(王珂), Shuai Chen(陈帅),Lifa Zhang(张力发), Yuxiang Ni(倪宇翔), and Gang Zhang(张刚)
Chin. Phys. B, 2023, 32 (**5**): 050505. DOI: 10.1088/1674-1056/acbaf0

Impact of counter-rotating-wave term on quantum heat transfer and phonon statistics in nonequilibrium qubit-phonon hybrid system

Chen Wang(王晨), Lu-Qin Wang(王鲁钦), and Jie Ren(任捷)
Chin. Phys. B, 2021, 30 (**3**): 030506. DOI: 10.1088/1674-1056/abcfa8

A polaron theory of quantum thermal transistor in nonequilibrium three-level systems

Chen Wang(王晨), Da-Zhi Xu(徐大智)
Chin. Phys. B, 2020, 29 (**8**): 080504. DOI: 10.1088/1674-1056/ab973b

Unifying quantum heat transfer and superradiant signature in a nonequilibrium collective-qubit system:A polaron-transformed Redfield approach

Xu-Min Chen(陈许敏), Chen Wang(王晨)
Chin. Phys. B, 2019, 28 (**5**): 050502. DOI: 10.1088/1674-1056/28/5/050502

Effect of temporal disorder on wave packet dynamics in one-dimensional kicked lattices

Yuting Wang(王雨婷), Yi Gao(高绎), Peiqing Tong(童培庆)
Chin. Phys. B, 2018, 27 (**12**): 120503. DOI: 10.1088/1674-1056/27/12/120503

Single-photon scattering and quantum entanglement of two giant atoms with azimuthal angle differences in a waveguide system

Jin-Song Huang(黄劲松)[1,†], Hong-Wu Huang(黄红武)[1], Yan-Ling Li(李艳玲)[1], and Zhong-Hui Xu(徐中辉)[2]

[1] *School of Information Engineering, Jiangxi University of Science and Technology, Ganzhou* 341000, *China*
[2] *Faculty of Science, Jiangxi University of Science and Technology, Ganzhou* 341000, *China*

(Received 20 December 2023; revised manuscript received 30 January 2024; accepted manuscript online 2 February 2024)

We theoretically investigate coherent scattering of single photons and quantum entanglement of two giant atoms with azimuthal angle differences in a waveguide system. Using the real-space Hamiltonian, analytical expressions are derived for the transport spectra scattered by these two giant atoms with four azimuthal angles. Fano-like resonance can be exhibited in the scattering spectra by adjusting the azimuthal angle difference. High concurrence of the entangled state for two atoms can be implemented in a wide angle-difference range, and the entanglement of the atomic states can be switched on/off by modulating the additional azimuthal angle differences from the giant atoms. This suggests a novel handle to effectively control the single-photon scattering and quantum entanglement.

Keywords: quantum transport, quantum entanglement, scattering theory, optical waveguide

PACS: 05.60.Gg, 03.65.Ud, 03.65.Nk, 42.79.Gn **DOI:** 10.1088/1674-1056/ad2508

1. Introduction

Manipulating photon transport in low-dimensional waveguides has motivated increasing interest owing to its extensive applications in quantum optics and quantum information.[1–3] In the past decades, waveguide quantum electrodynamics (wQED) systems,[4] which can tailor effectively the coupling between one-dimensional waveguide modes and quantum emitters, have provided powerful platforms to investigate the photon scattering. Based on such ideal platforms, a wide variety of striking transport properties in one-dimensional waveguides have been demonstrated, including asymmetrical Fano-line shapes,[5–8] electromagnetically induced transparency without control light field,[9–11] waveguide-mediated quantum entanglement,[12–15] unconventional photon blockade,[16–19] high-efficiency quantum routing and frequency conversion,[20–25] generating photonic band structures and bound states,[26–28] etc.

Generally, in a wQED system the coupled atom is usually regarded as a mass point due to the fact that its size is incomparable with the wavelength of the propagating mode in the waveguide. However, an emitter called giant atom,[29] which can couple to a waveguide at multiple separate connecting points, has attracted intensive attention recently since the atomic size is no longer negligible and ever parallel with the travelling-field wavelength. In contrast to single-point couplings of the familiar small atoms, the multiple-point couplings of the giant atoms will generate additional interference effects, and thus result in numerous exotic phenomena such as multi-frequency Fano resonance,[30–32] tunable nonreciprocal scattering,[33–35] phase-modulated Autler–Townes splitting,[36] and dynamical spontaneous emission.[37]

Surface plasmon transport in one-dimensional cylindrical nanowire waveguide has also attracted much attention in the nanophotonic field in recent years, owing to its great similarity to light transmission in usual dielectric optical components.[38,39] A recent interesting report[40] shows that the phase difference between two quantum dots in a plasmonic waveguide can be determined not only by the separation of quantum emitters coupled to the cylindrical waveguide, but also by the azimuthal angle difference between two emitters. Consequently, the azimuthal angle is also taken into account as a controllable variable, and has been utilized to perform the the Fano resonances in the scattering spectra and high concurrences of the entangled states.[41–43]

Inspired by these advances, we study the scattering properties of single photons and quantum entanglement between two giant atoms with four azimuthal angles in a cylindrical waveguide. By using a real-space Hamiltonian, the transmission and reflection amplitudes of the single photons are obtained analytically. Numerical results show that for the single-atom case, the single-photon transmission can be manipulated by tuning the azimuthal angle difference between two connecting points of the single atom, and zero transmissions related to the angle differences can be performed as tunable switches. For the two-atom case, asymmetric Fano-line shapes in the transmission spectra can emerge under the joint effects of the azimuthal angle differences from the additional inner- and inter-connecting points of two giant atoms, and the usual limits of equal atom-waveguide coupling and negative detuning are removed, in contrast to the previous scheme without the azimuthal angles.[5] High entanglement for two atoms is

[†]Corresponding author. E-mail: jshuangjs@126.com

© 2024 Chinese Physical Society and IOP Publishing Ltd

obtainable in a wide angle-difference scope, and the entangled state and unentangled state can be switched by tuning the azimuthal angle differences. Therefore, the proposed system may provide potential applications to modulate the photon transport and quantum entanglement in quantum communication.

2. Theoretical model

As displayed in Fig. 1, the considered structure is composed of two separate two-level giant atoms and a cylindrical waveguide, and each atom couples to the waveguide through two connecting points. The first giant atom couples to the waveguide at two locations $(x,\varphi)=(d_1,\phi_1)$ and (d_2,ϕ_2), respectively, while the second giant atom interacts with the waveguide at (d_3,ϕ_3) and (d_4,ϕ_4), respectively. Here, $x=d_m$ $(m=1,2,3,4)$ is the distance of these coupling points along the $\hat{x}$ axis direction of the waveguide, and $\varphi=\phi_m$ is the azimuthal angle for these coupling points of two twisted atoms along the $\hat{\varphi}$ direction of the surrounded waveguide. Since the forward guided-wave mode moves along the $\hat{x}$ and $\hat{\varphi}$ directions, the related phase difference between two neighboring connection points can be described as $\mathrm{i}kx+\mathrm{i}n\varphi$,[41] where k and n denote the wavenumber of the incoming photons and quantum number engineering the x and φ components, respectively. Each of the atoms is a two-level system characterized by the ground state $|g_j\rangle$ $(j=1,2)$ and excited state $|e_j\rangle$, with the transition frequency ω_j and the atomic dissipation rate γ_j. When a single photon is injected into the waveguide, the propagating wave is transmitted or reflected by these two giant atoms.

Under the rotating wave approximation, the real-space Hamiltonian[1,2] describing the coupled system can be written as ($\hbar=1$ hereafter)

$$\begin{aligned}H=&\iint \mathrm{d}x\mathrm{d}\varphi\Big\{-\mathrm{i}\upsilon_{\mathrm{g}}C_{\mathrm{R}}^{\dagger}(x,\varphi)\frac{\partial}{\partial x}C_{\mathrm{R}}(x,\varphi)\\&+\mathrm{i}\upsilon_{\mathrm{g}}C_{\mathrm{L}}^{\dagger}(x,\varphi)\frac{\partial}{\partial x}C_{\mathrm{L}}(x,\varphi)+\sum_{p=1,2}V_1\delta(x-d_p)\delta(\varphi-\phi_p)\\&\times\{[C_{\mathrm{R}}^{\dagger}(x,\varphi)+C_{\mathrm{L}}^{\dagger}(x,\varphi)]\sigma_{-}^{(1)}+[C_{\mathrm{R}}(x,\varphi)+C_{\mathrm{L}}(x,\varphi)]\sigma_{+}^{(1)}\}\\&+\sum_{q=3,4}V_2\delta(x-d_q)\delta(\varphi-\phi_q)\{[C_{\mathrm{R}}^{\dagger}(x,\varphi)+C_{\mathrm{L}}^{\dagger}(x,\varphi)]\sigma_{-}^{(2)}\\&+[C_{\mathrm{R}}(x,\varphi)+C_{\mathrm{L}}(x,\varphi)]\sigma_{+}^{(2)}\}\Big\}\\&+\sum_{p=1,2}(\omega_p-\mathrm{i}\frac{\gamma_p}{2})\sigma_{+}^{(n)}\sigma_{-}^{(n)}.\end{aligned}\tag{1}$$

Here, υ_{g} is the group velocity of the propagating photon; $C_{\mathrm{L}}^{(\dagger)}(x,\varphi)$ $[C_{\mathrm{L}}(x,\varphi)]$ and $C_{\mathrm{R}}^{(\dagger)}(x,\varphi)$ $[C_{\mathrm{R}}(x,\varphi)]$ are the bosonic operators of creating (annihilating) a left (right)-moving photon in the waveguide at the position x and with the azimuthal angle φ; $\sigma_{+}^{(p)}=|e_p\rangle\langle g_p|$ and $\sigma_{-}^{(p)}=|g_p\rangle\langle e_p|$ denote the raising and lowering operators for the p-th atom, respectively. The delta functions $\delta(x-d_m)$ and $\delta(\varphi-\phi_m)$ indicate that the atom-waveguide interactions occur at $x=d_m$ and $\varphi=\phi_m$, respectively. $V_{1(2)}$ denotes the atom-waveguide coupling strength.

Assuming that a single photon with the energy $\omega=\upsilon_{\mathrm{g}}k$ is input from the left port of the waveguide, the scattering eigenstate of the system can be expressed in the single-excitation subspace as

$$\begin{aligned}|\psi\rangle=&\iint \mathrm{d}x\mathrm{d}\varphi[\vartheta_{\mathrm{R}}(x,\varphi)C_{\mathrm{R}}^{\dagger}(x,\varphi)+\vartheta_{\mathrm{L}}(x,\varphi)C_{\mathrm{L}}^{\dagger}(x,\varphi)]|\emptyset\rangle\\&+u_1\sigma_{+}^{(1)}|\emptyset\rangle+u_2\sigma_{+}^{(2)}|\emptyset\rangle.\end{aligned}\tag{2}$$

Here, $|\emptyset\rangle=|0_{\mathrm{R}},0_{\mathrm{L}},g_1,g_2\rangle$ stands for the vacuum state of zero photons in the waveguide and the ground states for two giant atoms; u_1 and u_2 denote the excitation amplitudes of two atomic excited states, respectively; $\vartheta_{\mathrm{R}}(x,\varphi)$ and $\vartheta_{\mathrm{L}}(x,\varphi)$ are separately the wave functions of the right- and left-propagating photons in the waveguide. They take the following forms:

$$\begin{aligned}\vartheta_{\mathrm{R}}(x,\varphi)=&\,\mathrm{e}^{\mathrm{i}kx}\mathrm{e}^{\mathrm{i}n\varphi}[\theta(d_1-x)+t_1\theta(x-d_1)\theta(d_2-x)\\&+t_2\theta(x-d_2)\theta(d_3-x)+t_3\theta(x-d_3)\theta(d_4-x)\\&+t\theta(x-d_4)],\\\vartheta_{\mathrm{L}}(x,\varphi)=&\,\mathrm{e}^{-\mathrm{i}kx}\mathrm{e}^{-\mathrm{i}n\varphi}[r\theta(d_1-x)+r_1\theta(x-d_1)\theta(d_2-x)\\&+r_2\theta(x-d_2)\theta(d_3-x)+r_3\theta(x-d_3)\theta(d_4-x)],\end{aligned}\tag{3}$$

where $\theta(x)$ is the Heaviside step function, with $\theta(0)=1/2$; t and r are separately the transmission and reflection amplitudes in the waveguide; t_j and r_j denote the probability amplitudes for right-moving and left-moving photons between $x=d_j$ and $x=d_{j+1}$ $(j=1,2,3)$ in the waveguide, respectively.

Solving the eigenvalue equation $H|\psi\rangle=\omega|\psi\rangle$, we obtain

$$\begin{aligned}r=&-\Big[\mathrm{i}\Gamma_1(\mathrm{e}^{\alpha_1}+\mathrm{e}^{\alpha_2})^2B+\mathrm{i}\Gamma_2(\mathrm{e}^{\alpha_3}+\mathrm{e}^{\alpha_4})^2A\\&+2\sqrt{\Gamma_1\Gamma_2}D(\mathrm{e}^{\alpha_1}+\mathrm{e}^{\alpha_2})(\mathrm{e}^{\alpha_3}+\mathrm{e}^{\alpha_4})\Big]\cdot\left[AB+D^2\right]^{-1},\\t=&\,1-\Big[\mathrm{i}\Gamma_1(2+\mathrm{e}^{\alpha_1-\alpha_2}+\mathrm{e}^{\alpha_2-\alpha_1})B\\&+\mathrm{i}\Gamma_2(2+\mathrm{e}^{\alpha_4-\alpha_3}+\mathrm{e}^{\alpha_3-\alpha_4})A+D^2+DD^*\Big]\cdot\left[AB+D^2\right]^{-1},\\u_1=&\,\frac{V_1(\mathrm{e}^{\alpha_1}+\mathrm{e}^{\alpha_2})B-\mathrm{i}V_2(\mathrm{e}^{\alpha_3}+\mathrm{e}^{\alpha_4})D}{AB+D^2},\\u_2=&\,\frac{V_2(\mathrm{e}^{\alpha_3}+\mathrm{e}^{\alpha_4})A-\mathrm{i}V_1(\mathrm{e}^{\alpha_1}+\mathrm{e}^{\alpha_2})D}{AB+D^2},\end{aligned}\tag{4}$$

where $A=\Delta\omega+\mathrm{i}\gamma_1+2\mathrm{i}\Gamma_1(1+\mathrm{e}^{\alpha_2-\alpha_1})$, $B=\Delta\omega+\omega_{12}+\mathrm{i}\gamma_2+2\mathrm{i}\Gamma_2(1+\mathrm{e}^{\alpha_4-\alpha_3})$, $D=\sqrt{\Gamma_1\Gamma_2}(\mathrm{e}^{\alpha_3-\alpha_2}+\mathrm{e}^{\alpha_4-\alpha_2}+\mathrm{e}^{\alpha_3-\alpha_1}+\mathrm{e}^{\alpha_4-\alpha_1})$, $\Gamma_1=V_1^2/\upsilon_{\mathrm{g}}$, $\Gamma_2=V_2^2/\upsilon_{\mathrm{g}}$, and $\alpha_m=\mathrm{i}kd_m+\mathrm{i}n\phi_m$. $\Delta\omega=\omega-\omega_1$ is the frequency detuning between the incident photon and the first atom; $\omega_{12}=\omega_1-\omega_2$ is the frequency detuning between two emitters.

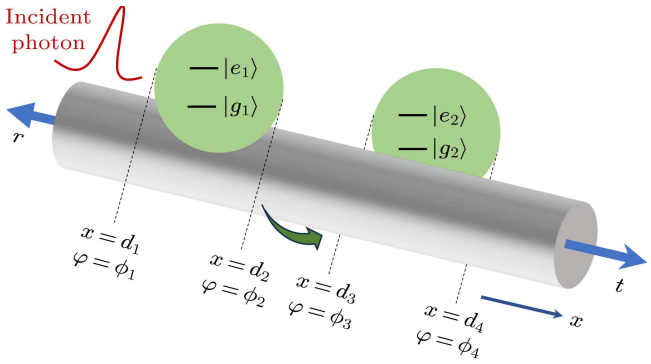


Fig. 1. Schematic configuration of scattering single photons along a waveguide by two giant atoms.

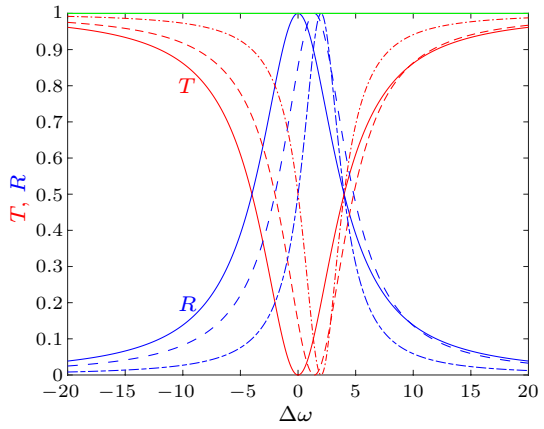


Fig. 2. Transmission probabilities T (red curves) and reflection probabilities R (blue curves) of the photons scattered by two atoms with different azimuthal angle differences: $\phi_2 = 0$ for solid curves, $\phi_2 = \pi/4$ for dashed curves, and $\pi/2$ for dash dotted curves. Here, $\phi_1 = 0$ and $\gamma_1 = 0$ are assumed, $kd_m = 2(m-1)\pi$ is fixed. For convenience, all parameters are in units of Γ_1 except the angles.

3. Scattering of single photons via two giant atoms

The transport properties of the single photons in the waveguide system are engineered by the transmission probability $T = |t|^2$ and reflection $R = |r|^2$. As a contrast, we first examine the single-atom case, in which the reduced coupling $\Gamma_2 = 0$ is assumed. Figure 2 displays the reflection spectra with the Lorentzian line shapes as a function of the frequency detuning $\Delta\omega$. Three reflection peaks approaching 1 emerge at the resonance points $\Delta\omega = 2\Gamma_1 \sin(\phi_2 - \phi_1)$, while these transmissions are completely blocked at the resonance locations. Notice that the conservation relation of the photon flow $T + R = 1$ (see green straight line) is on hold in two ports, when no dissipations are included. One can find that the resonance points can be modified by adjusting the azimuthal angle difference $\phi_2 - \phi_1$ from two-point couplings of the giant atoms, and relevant frequency shifts of the resonance points are presented for $\phi_2 = \pi/4$ and $\pi/2$. Here, $n = 1$ mode is set for the linear dispersion relation of guided wave, and $\phi_1 = 0$ is taken as the angle reference. For convenience, all parameters are in units of Γ_1 except the angles. Compared with the these results for small atom systems where the transmission is switched off at $\Delta\omega = 0$, the angle-dependent resonances can be implemented in tunable switchers of single photons.

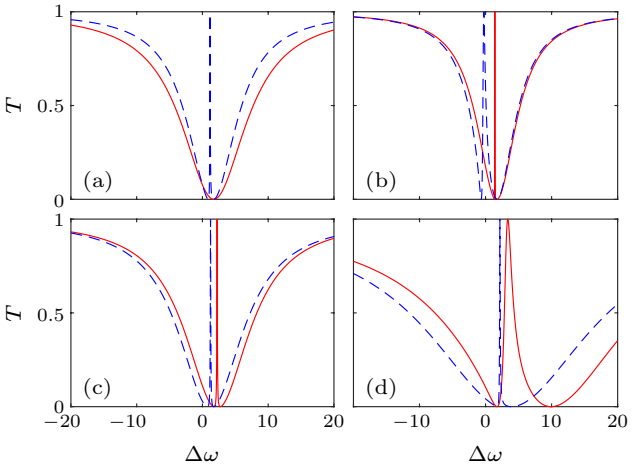


Fig. 3. Transmission T versus the detuning $\Delta\omega$: (a) $\omega_{12} = 0$, $\Gamma_2 = 1$ for red solid curve, and $\Gamma_2 = 0.5$ for blue dashed curve; (b) $\Gamma_2 = 0.2$, $\omega_{12} = -1$ for red solid curve, and $\omega_{12} = 1$ for blue dashed curve; (c) $\Gamma_2 = 1$, $\omega_{12} = -1$ for red solid curve, and $\omega_{12} = 1$ for blue dashed curve. (d) $\Gamma_2 = 4$, $\omega_{12} = -3$ for red solid curve, and $\omega_{12} = 3$ for blue dashed curve. Here, the parameters are taken as $\phi_2 - \phi_1 = \phi_4 - \phi_3 = \pi/3$, $\Delta\phi = \phi_3 - \phi_1 = 0$, and $\gamma_1 = \gamma_2 = 0$.

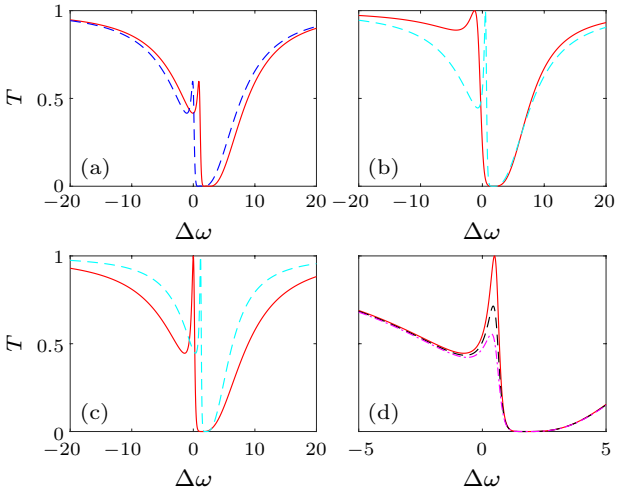


Fig. 4. Transmission T for different parameters: (a) $\phi_2 = \pi/3$, $\Delta\phi = \pi/8$, $\omega_{12} = -1$ for red solid curve, and $\omega_{12} = 1$ for blue dashed curve; (b) $\omega_{12} = 0$, $\phi_2 = \pi/3$, $\Delta\phi = \pi/4$ for red solid curve, and $\Delta\phi = \pi/8$ for cyan dashed curve; (c) $\omega_{12} = 0$, $\Delta\phi = \pi/8$, $\phi_2 = \pi/4$ for red solid curve, and $\phi_2 = \pi/2$ for cyan dashed curve; (d) $\omega_{12} = 0$, $\phi_2 = \pi/3$, $\Delta\phi = \pi/8$, $\gamma = 0$ for solid curve, $\gamma = 0.05$ for dashed curve, and $\gamma = 0.1$ for dash dotted curve. Other parameters are $\Gamma_2 = 1$ and $\gamma = \gamma_1 = \gamma_2 = 0$ in (a)–(c).

Next, we consider how the azimuthal angle affects the scattering spectra in the two-atom case. For simplicity, hereafter we consider that the two giant atoms have the same azimuthal angle differences $\phi_2 - \phi_1 = \phi_4 - \phi_3$ between their inner neighboring connection points, and $\Delta\phi = \phi_3 - \phi_1$ is the azimuthal angle difference from the first connection points of two atoms, which describes the angular torsion between two atoms. When we focus on $\Delta\phi = 0$, Fano-line shape appears for unequal atom-waveguide couplings $\Gamma_2 = 0.5\Gamma_1$, but the angle difference does not work to generate Fano-like resonance for zero detuning $\omega_{12} = 0$ and equal coupling $\Gamma_2 = \Gamma_1$ in

Fig. 3(a). However, the asymmetric Fano-type spectra with the resonance peaks can emerge even for equal atom-waveguide couplings and negative detunings, as shown in Figs. 3(b)–3(d), which is different from the condition of unequal atom-waveguide couplings and non-negative inter-atom detunings to result in Fano-like resonance in Ref. [5]. The underlying physics can be explained as follows: Fano-like resonance arises from the quantum inference between the localization and delocalization channels, where the localized channel is described by the single mode of coupling one atom with the photons, and the delocalized channel is described by the hybrid mode of coupling two atoms with the photons.[41] For zero detuning and equal coupling in Fig. 3(a), the overlapping of two peaks makes these two identical atoms jointly behave like a single atom, which means that the Fano-type line shape can not emerge owing to the lack of hybridization mode. For different atoms, Fano-like resonance occurs due to the quantum inference between two different channels.

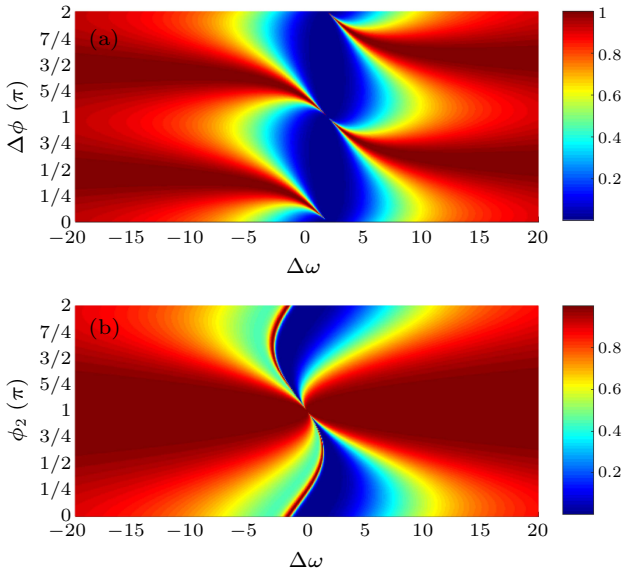


Fig. 5. Transmission T as a function of the detuning and the azimuthal angle difference: (a) $\phi_2 = \pi/8$, (b) $\Delta\phi = \pi/3$. Other parameters are $\Gamma_2 = 1$, $\omega_{12} = 0$, and $\gamma = 0$.

Furthermore, in Fig. 4 we plot the transmission profiles at different angle differences $\Delta\phi$ for the equal couplings $\Gamma_1 = \Gamma_2$. We find that the asymmetric Fano-line shapes characterized by the resonance peaks appear not only for $\omega_{12} = \pm 1$ in Figs. 4(a) but for zero detuning $\omega_{12} = 0$ in Figs. 4(b) and 4(c), which removes the restriction of zero detuning. Although $\Gamma_1 = \Gamma_2$ and $\omega_{12} = 0$ here, the different azimuth angles separate the two transmission peaks, and thus the quantum interference from these photons carrying two different angle phases can also occur by passing through the two interference channels. Varying the angle difference $\Delta\phi$ from $\pi/4$ to $\pi/8$, sharp Fano-type peak becomes more evident for the small $\Delta\phi$. To investigate the effect of the dissipations on transport properties, we show the transmission spectra in Fig. 4(d) for different dissipations. As is seen, with the increase of the dissipations, small amplitude Fano-line shape appears. Although the dissipations lead to lower probabilities of these Fano peaks, their behavior remains similar.

To gain a deeper insight into the effect of angle differences on the photon scattering, Fig. 5 shows the transmission versus the detuning $\Delta\omega$ and the angle differences ϕ_2 and $\Delta\phi$, where $\phi_1 = 0$ is fixed as a reference. As is seen, antisymmetric profiles are exhibited in two planes, and slender dark-red regions for perfect transmission peaks and oblate deep-blue windows for zero reflections can be applied to the design of switches. Figure 5(a) displays the Fano peaks at the sharp protrusions in a small scope of $\Delta\phi$ around $\pi/8$, while the narrow S-shaped stripe corresponding to Fano peaks occurs in almost the entire angular range of ϕ_2, as shown in Fig. 5(b).

4. Quantum entanglement of two giant atoms

In principle, the scattering photons traveling along the waveguide can be detected at two ends of the waveguide. However, if the incoming photon is not scattered but confined in two two-level atoms (qubits), the wave function can be projected onto the state $u_1|g_1, e_2\rangle|0_R, 0_L\rangle + u_2|e_1, g_2\rangle|0_R, 0_L\rangle$, which indicates that the entanglement between two atoms is created. The degree of entanglement can be characterized by the concurrence C of two qubits. In the proposed system, the density matrix of the Bell-like state is a pure-state density matrix, and thus the concurrence[5] is given by

$$C = \frac{2|u_1||u_2|}{|u_1|^2 + |u_2|^2}. \tag{5}$$

Figures 6(a) and 6(b) show separately the concurrence C and the populations $P_1 = |u_1|^2/(|u_1|^2 + |u_2|^2), P_2 = |u_2|^2/(|u_1|^2 + |u_2|^2)$ of two qubits, with and without the parameter of the azimuthal angle difference. As is seen, when one population of qubit 1 reduces, another of qubit 2 will increase, since the total population has always been 1. Correspondingly, the Fano-like occurrence of the maximum entanglement occurs when the populations of the two qubits are equal. To further study the effect of the azimuthal angle on the entanglement of two qubits, we plot the concurrence as a function of the detuning $\Delta\omega$ and the azimuthal angle difference ϕ_2 in Fig. 6(c). The concurrence does not have the periodicity, even though $\Delta\phi = \phi_2$ is assumed. The irregular dark-red rings indicating high entanglement are represented in a large angular range, while two dark-blue dips corresponding to zero concurrences emerge near $\phi_2 = \pi$. Moreover, the concurrences with the maximum approaching unity and the minimum close to 0 can appear at one same frequency by changing the azimuthal angle difference, which can be utilized to switch the maximally entangled and unentangled states via the azimuthal angle difference.

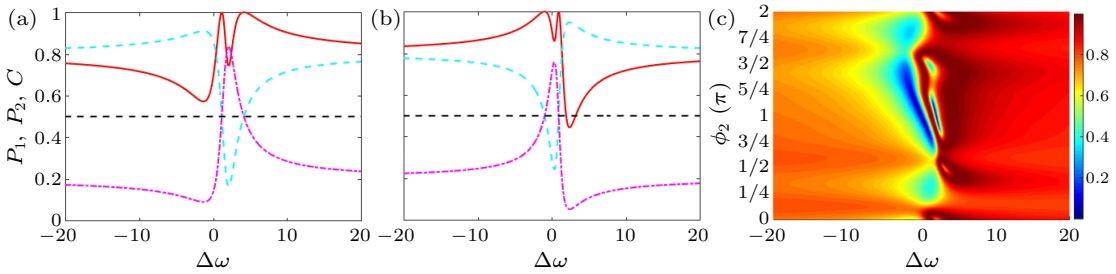


Fig. 6. Concurrence C (red solid curves), population P_1 (cyan dashed curves) and population P_2 (magenta dash dotted curves) of two qubits for different parameters: (a) $\omega_{12} = -2$ and $\phi_2 = \Delta\phi = 0$; (b) $\omega_{12} = 0$, $\phi_2 = \pi/2$, and $\Delta\phi = \pi/8$. Concurrence C as a function of ϕ_2 and $\Delta\omega$ in (c). Here $\omega_{12} = -2$ and $\Delta\phi = \pi/8$. The other parameter is $\Gamma_2 = 0.5$.

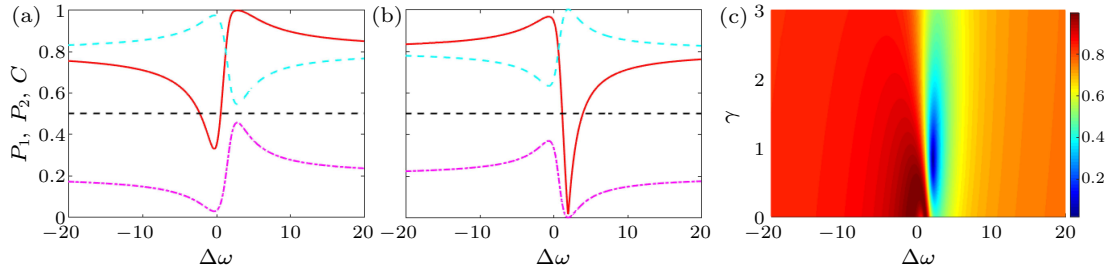


Fig. 7. Effect of the dissipations on the concurrence of two qubits for $\gamma = \gamma_1 = \gamma_2 = 0.8$, other parameters and the linetypes are the same as those in Fig. 6.

When the dissipations are included, the entanglement between two qubits will be suppressed, but the high entanglement with the concurrence peak approaching one can be kept ever for the larger dissipation such as $\gamma = 0.8$ in Fig. 7(a). Figure 7(b) displays that the Fano peak less than 1 occurs for the different populations due to the losses, and approaching zero concurrence without entanglement emerges when one qubit is non-populated. Figure 7(c) further shows the effect of the dissipations on the concurrence in a $(\Delta\omega, \gamma)$ plane. As the dissipation increases, high entanglement in the dark-red curved area gradually decreases, and a dip of the occurrence near zero value appears in the center of a blue ellipse region.

5. Conclusions

In summary, we have studied the scattering properties of the photons propagating in a waveguide system and quantum entanglement between two giant atoms with azimuthal angle differences coupled to the waveguide. For the single-atom case, the resonance point of the perfect reflection related to the angle difference is obtained, which can be used in the tunable switch. For the double-atom case, the Fano-line shape in the transmission spectra can be generated by varying the azimuthal angle difference, without the common limit of equal atom-waveguide coupling and negative detuning. High entanglement for two atoms is available, and two states between high and low entanglements can be switched by changing the azimuthal angle difference. The influence of the dissipations on the entanglement has also been analyzed. These results suggest a new way to control the transport and entanglement, which may be utilized in quantum communication.

Acknowledgments

Project supported by the National Natural Science Foundation of China (Grant Nos. 12365003, 12364024, and 11864014) and the Jiangxi Provincial Natural Science Foundation (Grant Nos. 20212BAB201014 and 20224BAB201023).

References

[1] Shen J T and Fan S 2005 *Phys. Rev. Lett.* **95** 213001
[2] Shen J T and Fan S 2009 *Phys. Rev. A* **79** 023837
[3] Zhou L, Gong Z R, Liu Y X, Sun C P and Nori F 2008 *Phys. Rev. Lett.* **101** 100501
[4] Goban A, Hung C L, Yu S P, Hood J D, Muniz J A, Lee J H, Martin M J, McClung A C, Choi K S, Chang D E, Painter O and Kimble H J 2014 *Nat. Commun.* **5** 3808
[5] Chen G Y, Liu M H and Chen Y N 2014 *Phys. Rev. A* **89** 053802
[6] Mukhopadhyay D and Agarwal G S 2019 *Phys. Rev. A* **100** 013812
[7] Mukhopadhyay D and Agarwal G S 2020 *Phys. Rev. A* **101** 063814
[8] Shu Y X, Ma X S, Huang X S, Cheng M T and Han J B 2021 *Chin. Phys. B* **30** 104204
[9] Mukhopadhyay D and Agarwal G S 2020 *Phys. Rev. A* **101** 063814
[10] Zheng H X and Baranger H U 2013 *Phys. Rev. Lett.* **110** 113601
[11] Jia W Z and Cai Q Y 2022 *Eur. Phys. J. Plus* **137** 1082
[12] Zheng H X and Baranger H U 2013 *Phys. Rev. Lett.* **110** 113601
[13] Gonzalez-Ballestero C, Moreno E and Garcia-Vidal F J 2014 *Phys. Rev. A* **89** 042328
[14] Facchi P, Kim M S, Pascazio S, Pepe F V, Pomarico D and Tufarelli T 2016 *Phys. Rev. A* **94** 043839
[15] Liu A P, Cheng L Y, Guo Q, Su S L, Wang H F and Zhang S 2022 *Chin. Phys. B* **31** 080307
[16] Zhang X Q, Xia X W, Xu J P, Li H Z and Fu Z Y 2022 *Chin. Phys. B* **31** 074204
[17] Chen M Y, Tang J S, Tang L, Wu H D and Xia K Y 2022 *Phys. Rev. Res.* **4** 033083
[18] Feng L J, Yan L and Gong S Q 2023 *Front. Phys.* **18** 12304
[19] Sun J Y and Shen H Z 2023 *Phys. Rev. A* 107 043715
[20] Zhou L, Yang L P, Li Y and Sun C P 2013 *Phys. Rev. Lett.* **111** 103604
[21] Liu A P, Cheng L Y, Guo Q, Su S L, Wang H F and Zhang S 2019 *Chin. Phys. B* **28** 020301
[22] Zhang J H, He D Y, Luo G Y, Wang B D and Huang J S 2021 *Chin. Phys. B* **30** 034204
[23] Liu J S, Yang Y, Lu J and Zhou L 2022 *Chin. Phys. B* **31** 110301

[24] Jia W Z, Wang Y W and Liu Y X 2017 *Phys. Rev. A* **96** 053832
[25] Cao M S and Jia W Z 2021 *J. Phys. B* **54** 055502
[26] Ai Q and Liao J Q 2010 *Commun. Theor. Phys.* **54** 985
[27] Ahumada M, Orellana P A and Retamal J C 2018 *Phys. Rev. A* **98** 023827
[28] Talukdar J and Blume D 2018 *Phys. Rev. A* **108** 023702
[29] Kannan B, Ruckriegel M J, Campbell D L, Kockum A F, Braumüller J, Kim D K, Kjaergaard M, Krantz P, Melville A, Niedzielski B M, Vepsäläinen A, Winik R, Yoder J L, Nori F, Orlando T P, Gustavsson S and Oliver W D 2020 *Nature* **583** 7818
[30] Feng S L and Jia W Z 2021 *Phys. Rev. A* **104** 063712
[31] Peng Y P and Jia W Z 2023 *Phys. Rev. A* **108** 043709
[32] Liu J Y, Jin J W, Liu H Y, Ming Y and Yang R C 2023 *Quantum Inf. Process.* **22** 74
[33] Liu N, Wang X, Wang X, Ma X S and Cheng M T 2022 *Opt. Express* **30** 23428
[34] Chen Y T, Du L, Guo L Z, Wang Z H, Zhang Y, Li Y and Wu J H 2022 *Commun. Phys.* **5** 215
[35] Wang X, Yang W X, Chen A X, Li L, Shui T, Li X Y and Wu Z 2022 *Quantum Sci. Technol.* **7** 015025
[36] Zhao W, Zhang Y and Wang Z H 2022 *Front. Phys.* **17** 42506
[37] Du L, Zhang Y and Li Y 2022 *Front. Phys.* **18** 12301
[38] Wei H, Pan D, Zhang S P, Li Z P, Li Q, Liu N, Wang W H and Xu H X 2018 *Chem. Rev.* **118** 2882
[39] Guo X, Ma Y G, Wang Y P and Tong L M 2013 *Laser Photon. Rev.* **7** 855
[40] Li Q, Wei H and Xu H X 2014 *Nano Lett.* **14** 3358
[41] Kuo P C, Chen G Y and Chen Y N 2016 *Sci. Rep.* **6** 37766
[42] Huang J S, Zhang J H, Wang Y, Xu Z H and Huang Y W 2018 *Opt. Commun.* **419** 25
[43] Ryom J S, Kim N C, Ko M C and Choe S I 2022 *Plasmonics* **17** 949